Accepted Manuscript

The impedance analysis of sintered $MgTiO_3$ ceramics

S. Filipović, V.P. Pavlović, N. Obradović, V. Paunović, K. Maca, V.B. Pavlović

PII: S0925-8388(17)30140-8

DOI: 10.1016/j.jallcom.2017.01.117

Reference: JALCOM 40484

To appear in: *Journal of Alloys and Compounds*

Received Date: 13 December 2016

Revised Date: 10 January 2017

Accepted Date: 14 January 2017

Please cite this article as: S. Filipović, V.P. Pavlović, N. Obradović, V. Paunović, K. Maca, V.B. Pavlović, The impedance analysis of sintered $MgTiO_3$ ceramics, *Journal of Alloys and Compounds* (2017), doi: 10.1016/j.jallcom.2017.01.117.

The impedance analysis of sintered $MgTiO_3$ ceramics

S. Filipović[1], V. P. Pavlović[2], N. Obradović[1,*], V. Paunović[3], K. Maca[4], V. B. Pavlović[1]

[1]Institute of Technical Science of SASA, 11000 Belgrade, Serbia
[2]Faculty of Mechanical Engineering, University of Belgrade, 11000 Belgrade, Serbia
[3] Faculty of Electronic Engineering, University of Nis, 18000 Nis, Serbia
[4]CEITEC BUT, Brno University of Technology, 61600 Brno, Czech Republic

Abstract

In the present study the effect of preparation conditions on microstructure and electrical properties of $MgTiO_3$ ceramics was investigated. Mixture of MgO and TiO_2 powders was subjected to mechanical activation for different time periods. Two types of sintering (two-step and HIP sintering) were performed on green bodies prepared by cold isostatic pressing. AC impedance spectroscopy in the low-frequency range (from 20 Hz to 1 MHz), at room and elevated temperatures, were performed in order to separate contribution of grains and grain boundaries to capacitance, resistance and conductivity of magnesium titanate ceramics. The special attention was directed to explanation of the influence of mechanical activation on electrical and morphological changes in sintered samples. The significant decrease of partial oxygen pressure in HP sintering atmosphere caused the change from insulating behavior of $MgTiO_3$ samples after two-step sintering to semiconducting one.

Keywords: mechanical activation, AC impedance analysis, SEM, titanate-based ceramics.

1. Introduction

In the MgO-TiO_2 binary system, a few compounds could be found, depending mainly on the molar ratio of starting oxides. Two of them, $MgTiO_3$ and Mg_2TiO_4, are stable and formed by a solid-state reaction [1]. Beside these two compounds, metastable $MgTi_2O_5$ phase is often present during $MgTiO_3$ formation by many synthesis methods [2].

In last few decades, the improvement in microwave dielectric materials is very important due to rapid development of modern communication devices, such as cellular telephones, antennas, and global positioning systems [3, 4]. $MgTiO_3$ is a material often used in fabrication of different type of resonators and capacitors, so enhancement of this material is still in focus of many research groups.

It is well known that preparation conditions influence significantly the final structure and electrical properties of ceramic materials. Important achievement is to obtain ceramic with nearly full density and fine grains with homogenous distribution [5]. The mechanical activation, as pretreatment for shaping and sintering process, is a very convenient way of powder preparation with uniform particle size distribution. Processes such as increase in the number of contacts and massive necks formation occur during early stage of sintering. The neck growth is controlled by numerous diffusion mechanisms with rates determined by the total flux of atoms coming to the neck, suggesting that dominant processes occurs at grain boundaries [6]. Similarly, many functional properties of ceramics also reflect the importance of grain boundaries. From that point of view, the electrical properties must be measured using AC techniques, so that the effects of grains and grain boundaries can be assessed separately. Furthermore, it is known that sintering conditions, such as temperature and atmosphere, could drastically change electrical properties, including transition from insulating to semiconducting behavior for titanate based materials [7].

*Corresponding author: nina.obradovic@itn.sanu.ac.rs (Dr. Nina Obradovic)

In this paper, the influence of mechanical activation along with sintering conditions on electrical properties of sintered $MgTiO_3$ electroceramic was reported. The impedance analysis was used to determine contribution of grains and grain boundaries to capacitance, resistance and conductivity of magnesium titanate based ceramics. Having in mind that there are no attempts of this kind of investigation for two-step and HIP sintered mechanically activated magnesium titanate ceramic, the obtained results are of wide interest, scientific and practical, as well.

2. Experimental procedure

In these experiments, commercial MgO and TiO_2 powders (Sigma–Aldrich, purity ≥ 99 %) were used, as initial reagents. Magnesium oxide, which usually contains $Mg(OH)_2$, was calcined at 700 ^oC for 2 h to remove hydroxide component, in order to achieve as accurate stoichiometry. The powder mixtures, in molar ratio 1:1, were ball milled in Fritsch Pulverisette 5 equipment, with ZrO_2 balls and vessels. The performed mass ratio of ball to powder was 40:1 and duration of mechanical treatment was varied from 0 to 160 min. Obtained powders mixtures were pressed in cylindrical specimens with applied isostatic pressure of 300 MPa.

Pressed samples were subjected to sintering process. The first set of specimens was two-step sintered with the following regime: heating up to 1300 ^oC with heating rate 10 ^oC/min, dwell for 30 minutes and cooling down with applied rate 5 ^oC/min, and then re-sintered up to 1200 ^oC with heating rate 20 ^oC/min, dwell for 20 h and cooling rate 10 ^oC/min. The two-step sintered samples were denoted as MT0-MT160, according to activation time.

The second experiment was obtained by applying combing sintering technique. In the first step, mechanically activated and pressed specimens were heated up to 1400 ^oC with heating rate 10 ^oC/min, hold for 30 min and after that, cooled down to room temperature. Only samples which achieved closed porosity were post-sintered by pressure assisted technique Hot Isostatic Pressing (HIP) at 1200 ^oC for 2 h in an argon atmosphere with pressure of 200 MPa (ABRA Shirp, Switzerland). The HIP sintered samples were denoted as HIP10-HIP160, according to activation time.

Electrical characteristics were measured using Agilent 4284A precision LCR meter in frequency range from 20 Hz to 1 MHz. The variations of electrical properties with temperature were measured in temperature interval from 20 to 180 ^oC. The samples were heated in temperature chamber Heraeus HEP2, which is fully automated. Prior to electrical measurements, silver paste was applied on flat surfaces of specimens.

3. Results and discussion

Fig. 1 presents the influence of mechanical activation on morphological changes of MT samples. Sintered process was performed in an air atmosphere, as it was described in the experimental part. For non-activated samples, the main characteristic is high level of open porosity, initially formation of contact necks, which is an indication of early sintering stage.

Fig. 1. Scanning electron micrographs of MT samples: a) MT0, b) MT10, c) MT40, d) MT80, and e) MT160.

The exposure to high mechanical energy during milling process leads to irreversible plastic deformation of the initial material and attrition of powder particles. A change in the size and structure of the particles during mechanical activation causes instability of treated powders, which is reflected in the changed sinterability of samples, within the applied sintering regime, and finally in changes of their final structure [8]. Therefore, samples MT10 and MT40 exhibit significantly lower level of open porosity, more compact structure, but with grains which retained their individuality (Fig.1b and c). This is a characteristic of intermediate sintering stage. Prolonged milling process, as sintering pretreatment, leads to formation of more uniform microstructure of starting powders, as described earlier [8]. This induced uniform grain distribution, spheroidization

of some pores and also strengthened grain boundaries, and fractures through grains. All mentioned changes in morphology are characteristic of the transition between the intermediate stage and the final sintering stage. Furthermore, the abnormal grain growth was avoided, the main goal of two-step sintering method, indicating an appropriate selection of sintering conditions.

Fig. 2. Scanning electron micrographs of HIP samples: a) HIP10, b) HIP40, c) HIP80, and d) HIP160.

Hot Isostatic Pressing is a useful method to produce compact and dense materials with densities near to theoretical values. Usually applied sintering temperature is significantly lower than in the case of pressure-less sintering techniques [9]. It is very important to emphasize that in case of capsule-free HIP the pre-sintering step is needed to ensure closed porosity within samples. In case of samples with pores that are not all closed, HIP sintering will not be effective [10]. It is the reason why non-activated sample not HIPed because it has not achieved closed porosity in pressure-less sintering regime. Micrographs of samples HIP10 and HIP40, presented in fig. 2a and b, indicate the presence of spiral-like growth features. For this type of crystal growth, each grain or column grows by molecules accumulation to a spirally expanding ramp on the grain surface in the classical curved growth mechanism. Such obtained screw dislocations will create steps in the surface, avoiding the inevitability for 2D nucleation [11]. Possible mechanism for forming screw dislocations may refer to incoherent meeting of two growth fronts, corresponding to MgO and TiO_2 components, which develop sufficiently and meet each other over an earlier grown structure. Higher level of lattice disorder and concentration of defects was noticed by careful investigation of Raman spectra for HIP samples, especially HIP10 and HIP40 samples, published previously [8]. For samples HIP80 and HIP160, fig. 2c and d, the main characteristic is grain growth along with fractures through grains and negligible content of spherical pores. Reducing particle size before HIP sintering significantly increased densification rate [9]. More uniform particle distribution with smaller grains observed in the powders activated for 80 and 160 min, produced much higher densities and much compact structure than those of the powders activated for shorter times [8].

The complex impedance technique is a very convenient method for detail study of the electrical response of sintered ceramics in wide frequency range. This method could be successfully applied to separate the contribution of electrical properties due to the bulk and grain boundary response. So, the effects of mechanical activation as well as sintering regime on electrical properties of magnesium titanate at different temperatures and frequencies are considered.

From diagrams in the Z* (fig. 3a) and Y* (fig. 3b) complex planes (Z* and Y* denote electrical impedance and admittance respectively, in complex form, where: $Y^* = \left(Z^*\right)^{-1}$), it could be concluded that HIP samples have significantly lower resistance than the two-step sintered MT samples. It has been observed at both room temperature and higher temperatures. Namely, the response of MT and HIP samples for any selected temperature cannot be seen on the same diagram, due to the large differences in the size ranks of the resistance of these samples. Therefore, only the curve corresponding to one or other sample group (MT or HIP) could be seen (figs. 3a and b). For example, the MT sample response is clearly visible in the Z* plane, while semicircles derived from HIP samples are well-defined in the Y* plane. Because of these significant differences between MT and HIP samples, they will be considered separately in the majority of the following diagrams.

At room temperature it was impossible to estimate the overall resistance of the MT samples and the individual contribution of the grain and the grain boundaries, from the Z* and Y* complex planes in the frequency range from 0.2 kHz to 1 MHz, so the main observation will be directed to highest applied temperature.

Figure 3. Plots in. a) Z* plane (Nyquist plots) and b) Y* plane, for all sintered samples.

In Z* plane in fig. 3a, only the vertical lines that correspond to the beginning of the semicircles associated to grain response for different MT patterns was noticed. In accordance with this is the fact that in the diagram of $Z'' = f(\nu)$ there are no peaks detected for MT samples (fig. 4a). So, in the applied frequency range, neither the total resistance for this set of samples nor the contribution of the grain and the grain boundaries to this resistance can be accurately estimated.

From diagrams $Y' = f(\nu)$ it can only be assessed that the total resistance of these samples are of the order of 10 GΩ, even at 180 ^{o}C, as seen in fig. 4b. This is in a good agreement with results published for magnesium titanate ceramics by other authors [12, 13]. The estimation was done in accordance with the basic impedance formalism, assuming that the electrical properties of the sample may be represented by a corresponding equivalent circuit composed of two circuits that simulate the impedance contribution of grains and contribution of grain boundaries, respectively [14].

Figure 4. Frequency dependence of: a) imaginary part of the complex impedance, b) real part of the complex admittance, at 180 ^{o}C, for two step sintered samples (MT0-MT160).

The analysis of data in M* complex plane (fig. 5), where M* is complex electric modulus, has shown that the MT capacitance values are much smaller order of magnitude than for the HIP samples. Although the figure shows the both spectra of HIP and MT samples, the former can not be seen because of the large differences in the capacitance order of magnitude for these groups of samples. Total capacitance of the MT samples has been estimated from the M* plane, not just at highest temperature, but also at room temperature.

Figure 5. Plots in M* plane for MT and HIP samples at: a) 180 ^{o}C and b) 30 ^{o}C

From data presented in figs. 6a and b, a pronounced decrease of capacitance with increasing temperature can be noticed for the activated MT samples, particularly for the activation time of 40 min. For longer activated samples, the mentioned effect is less pronounced. It is also detected that a capacitance decreases for the first 40 min of activation, than follows further increase up to the activation time of 100 min and finally manifests declining tendency again.

Figure 6. a) Plots in M* plane for MT samples at 180 ^{o}C and 30 ^{o}C, and b) the capacitance of MT samples at 30 ^{o}C and 180 ^{o}C vs. activation time.

Considering that the resistance of HIP patterns is much smaller than for MT samples, the value of the former could be assessed on the basis of impedance formalism in applied temperature and frequency range. It can be concluded from the fig. 7a that the observed HIP semicircles in Z* plane arise from the superposition of grains and grain boundaries resistance contribution. This can be inferred primarily from the asymmetry of semicircles assigned to samples HIP10 and HIP40. The asymmetry originates from the contribution of the grain resistance in the range of higher frequencies. Within increase of activation time from 10 to 40 min, diameter of the semicircle in Z* plane decreases, while with prolonged activation it moves towards higher values (fig. 7a), implying the analogue change of total resistance. All semicircles in the Z* plane are lowered, which is caused by non-Debye type of relaxation, which is common in polycrystalline samples due to the presence of porosity, defects on the grain boundaries, the possible presence of different phases, occurrence of a liquid phase, different types of grain boundaries and various types of pores, etc [14].

Figure 7. a) Plots in Z* plane (Nyquist plots) and b) frequency dependence of imaginary part of electrical impedance, for HIP sintered samples at 180 ^{o}C.

Mechanical activation has influenced the shift of the frequency corresponding to the maximum of the observed semicircles, towards lower values. This effect could be perceived through the displacement of the maximum of function $Z'' = f(\nu)$, in fig. 7b.

From extrapolation of the semicircles in the complex planes of electrical impedance and admittance, to their intersection with the abscissa (figs. 7a and 8a), total resistance of HIP samples has been calculated, as well as partial contribution of grain and grain boundaries resistance, at the highest applied temperature of 180 ^{o}C. Assessment of the total resistance is also carried out at room temperature, based on the cross section of the extrapolated semi-circular to the abscissa at the lowest frequencies range in Y* plane (fig. 8b).

Figure 8. Plots in Y* plane for HIP sintered samples at: a) 180 ^{o}C and b) 30 ^{o}C. Insets represent enlarged view of the results in the low frequency range.

The influence of mechanical activation on the total resistance of HIP samples is shown in fig. 9a. It is observed that with the increase of activation time up to 40 min the total resistance decreases, while for the longer activation time this trend is changed. The shifts of semicircles at diagrams in Z* plane have already indicated this trend of change in resistance. As it can be seen

from fig. 9a, total resistance of HIP sintered samples is a few orders of magnitude smaller then resistance of MT ones (estimated earlier to be around 10 GΩ). Magnitudes of resistance for HIP samples are indicating that this way prepared ceramic show semiconducting properties, while MT samples are insulating. This is obvious from fig. 9a, where with increasing temperatures from 30 ^{o}C to 180 ^{o}C the total resistance value decreases for one order of magnitude. Further, the color of MT samples was white, while color of HIP ones was black, indicating totally different behavior. It is known that the electrical property strongly depends on oxygen non-stoichiometry. The resistance is heavily dependent on the degree of re-oxidation that occurs during preparation of ceramic materials [7]. During HIP sintering, inert argon atmosphere induced lack of oxygen, according to equation:

$$2O_O^x \rightarrow O_2(g) + 2V_O^{\bullet\bullet} + 4e^- \quad (1)$$

Such formed electrons lead to reduction of Ti^{IV+} to Ti^{III+} and produce dark-colored, n-type semiconducting materials. Further, a higher concentration of defects occurred within this process also produces a higher conductivity for this type of materials [15]. Higher concentration of defects such as vacancies, electrons, and Ti^{III+} ions, are confirmed by Raman spectroscopy investigation, published previously [8].

Figure 9. a) Total resistance of HIP sintered samples as a function of activation time; b) the grains and grain boundaries resistance contribution for the HIP samples at 180 ^{o}C vs. activation time.

Contribution of grains and grain boundaries to resistance of the HIP samples was estimated from measurements obtained at 180 ^{o}C and the influence of activation time for these parameters is shown in fig. 9b. It was observed that the resistance of the grains (R_1) is considerably lower than the resistance of grain boundaries (R_2). Mechanical activation of the starting powders, associated with the HIP treatment led to significantly different values of electrical properties of components of grains and grain boundaries, than it is shown by authors X. Kuang et al [16]. Due to these reasons, consideration of our impedance spectra was performed in four complex plains: Z*, Y*, M*, and ε_r*. Generally, the appearance of "mutually merged semicircles", derived from grains and grain boundaries within the dielectric ceramic, is not unusual and it depends on the ratio of the characteristic time constants: τ_Z and τ_{GZ}. P. Gogoi et al [17] got one asymmetric semicircle in Z* plane, with the asymmetry in the range of high frequency for $MgTiO_3$ ceramics, as is the case in our spectra of prolonged activated samples. In the investigations performed by P. Gogoi et al, partial separation significantly smaller semicircle in the frequency area that corresponding to the grain was observed, at one of the studied temperatures, indicating that in this case the grains resistance for $MgTiO_3$ ceramic was considerably lower than the resistance of grain boundaries. Considering the semiconducting properties of HIP samples, one can notice that the similar kind of behavior was observed for $BaTiO_3$ ceramic sintered in an argon atmosphere [7], where it was shown that both grain and grain boundary responses were detected and both were semiconducting, as it was in our HIP sintered samples. However, for the Ar-annealed pellets, the grain boundaries became more insulating than the grains, possibly because of inhomogeneity of the microstructure owing to a limited re-oxidation along with the grain boundary region during the cooling procedure after the annealing process and in the electrode firing procedure in air, as it was explained by H. Zhu at al [15].

Based on the data obtained from Z* and Y* planes for HIP sintered samples at several temperatures, the influence of the activation time on the temperature dependence of resistance was investigated. In figs. 10 a-d, the influence of temperature on the diagrams in Z* and Y* planes for HIP10 and HIP40 samples are showed.

Figure 10. The influence of temperature on the diagrams in Z* and Y* planes for samples HIP10 and HIP40. Insets represent enlarged view of the results in the low frequency range.

The activation energy (E_a) for the conduction process in HIP sintered samples was determined from coefficient of direction in the graphic $\ln R = f(1/T)$, applying the Arrhenius

equation: $R = \beta e^{\frac{E_a}{kT}}$. The resistance estimated from extrapolation of the semicircles to their intersection with the abscissa at the lowest frequencies in the Z* and Y* planes were used for this purpose. The results are shown in fig. 11a, from which it could be seen that for activation up to 40 min the activation energy of conducting process decreases, while for the longer activation time its value increases.

Figure 11. Dependence $\ln R = f(1/T)$ for activated and HIP sintered samples (a). The frequency dependence of conductivity for HIP samples at 180 ^{o}C (b).

The main reason for this trend of change in the activation energy probably lies in heterogeneity of the microstructure, confirmed by SEM (fig. 2), especially for sample HIP10 and HIP40 where increase of number of dislocation was detected, as well as enhanced content of oxygen vacancy, Ti^{III+} and weakly bonded electrons, which are observed by Raman spectroscopy [8]. This increase in defect concentration enlarged conductivity within samples activated up to 40 min, and consequently reduced E_a values.

In fig. 11b, the frequency dependence of conductivity for HIP samples in the low range of frequencies is shown. Fitting was performed using the Jonscher's universal power law [18]: $\sigma_\omega = \sigma_0 + A\omega^n$. The impact of the activation time on the characteristic frequency parameter *n* and the DC value of conductivity (σ_0) was estimated from that and presented in the figure. It can be seen that the influence of the activation on σ_0 value is in accordance with the previously discussed impact of the activation time on the changes in the total resistance of the samples. According to K. Funke, the value $n > 1$ indicates the thermally generated conductivity of the patterns [19].

For HIP sintered samples, the influence of the activation time on the contribution of grain boundary capacitance was estimated from data in the complex modulus plane ($M^* = (\varepsilon^*)^{-1}$), by extrapolation of semicircle at the lower frequencies (fig. 12a).

Figure 12. Plots in: a) M* plane and b) ε_r * plane, for HIP sintered samples at 180 ^{o}C. Inset represents enlarged view of the results in the high frequency range; c) the contribution of grain boundary capacitance for the HIP sintered samples at 180 ^{o}C vs. activation time.

The obtained values were verified based on an extrapolation of a semicircle in the complex plane of relative permeability (ε_r*, fig. 12b) and are shown in fig. 12c. Estimated values for grain boundary capacitance are of the order of several nF, which is characteristic for this type of materials [16]. The presented trend of $C_2 = f(t_A)$ function is further confirmed on the bases of: a) the data for the resistance of grain boundaries and b) estimated frequencies values of the maximum of curves $M'' = f(\nu)$ in the range of lower frequencies (fig. 13). For this purpose we used the fact that in the idealized case (on the approximation of Debye relaxation), frequency which corresponds to the maximum of curve $M'' = f(\nu)$ in the lower frequencies range is associated with resistance and capacitance of the grain boundary component within the material (i.e. with the resistance and capacitance of the grain boundary element in the corresponding sub-circuit within the equivalent electrical circuit) via the relation: $\omega_m = 2\pi\nu_m = \frac{1}{\tau} = \frac{1}{RC}$ [14].

Figure 13. Frequency dependence of imaginary part of complex electric modulus for HIP10-HIP160 samples, measured at 180 ^{o}C.

It is known that semicircles corresponding to grain and grain boundaries are not well separated in Z* plane in materials with similar order of magnitude for capacitance contribution of grain and grain boundaries, as in the case of our samples [19]. Therefore, based on the data for HIP

samples in Z* plane, it was possible to assume that the capacitance of grains and grain boundaries are values of the similar order of magnitude, for all HIP sintered patterns.

4. Conclusion

In this paper, the influence of mechanical activation of powders along with sintering conditions on morphological changes and electrical properties of $MgTiO_3$ electroceramic was investigated. SEM and impedance analysis were used for this investigation.

The micrographs of two-step sintered samples (MT) indicated the increase in transport mass and more compact structure formation, with less content of open porosity, with prolonged mechanical treatment. For HIP sintered samples, the main characteristic was presence of spiral-like growth features within samples HIP10 and HIP40, and formation of screw dislocations.

Impedance analysis of MT samples showed that the total resistance of these samples is of the order of 10 GΩ, confirming insulating behavior. The capacitance of MT samples decreases for the activation up to 40 min, while for prolonged activation time this trend is changed.

HIP sintered samples show totally different behavior in the electrical properties. It is detected that Ar atmosphere, applied during this sintering method, switch this ceramics from insulating to semiconducting. The inert atmosphere induced lack of oxygen and such formed electrons lead to reduction of Ti^{IV+} to Ti^{III+} and produce dark-colored, n-type semiconducting materials. The resistance of both grain and grain boundary component in HIP sintered samples was estimated and both components have proved to be semiconducting. The samples obtained at shorter activation time (up to 40 min) have shown lower values of resistance and activation energy of conducting process, than samples produced from longer activated powders. Further, it is detected that degree of disorder in crystal structure and microstructure influences strongly the process of thermal conductivity, as well as changes in the activation energy.

From all presented correlations, it could be concluded that mechanical activation as well as sintering conditions strongly affect final electrical properties of magnesium titanate ceramic. Depending on the final application, appropriate preparation conditions could be chosen.

Acknowledgement

This research was performed within the project OI 172057 funded by the Ministry of Education, Science and Technological Development of the Republic of Serbia.

5. References

[1] A. Belous, O. Ovchar, D. Durylin, M. Valant, M. Macek-Krzmanac, D. Suvorov, Microwave composite dielectrics based on magnesium titanates, J. Eur. Ceram. Soc. 27 (2007) 2963–2966.

[2] K. Sreedhar, N.R. Pavaskar, Synthesis of $MgTiO_3$ and $Mg_4Nb_2O_9$ using stoichiometrically excess MgO, Mater. Lett. 53 (2003) 452–455

[3] A. Belous, O. Ovchar, D. Durilin, High-Q Microwave Dielectric Materials Based on the Spinel Mg_2TiO_4, J. Am. Ceram. Soc. 89 (2006) 3441–3445

[4] Z. Li, S. Chun-Ying, Q. Tai, Studies on the $(1-x)(Mg_{0.7}Zn_{0.3})TiO_3$ $xCa_{0.61}La_{0.26}TiO_3$ microwave dielectric ceramics system J. Inorg. Mater. 26 (2011) 219–224.

[5] S. Filipović, N. Obradović, V. B. Pavlović, D. Kosanović, M. Mitrić, N. Mitrović, V. Pouchly, M. Kachlik, K. Maca, Advantages of Combined Sintering Compared to Conventional Sintering of Mechanically Activated Magnesium Titanate, Science of Sintering, 46 (2014) 283-290.

[6] V. V. Mitic, V. Paunovic, V. Pavlovic, Lj Zivkovic, Sintering Process Influence on Microstructure and Intergranular Impedance of Rare-Earth Modified $BaTiO_3$-Ceramics, Sci. Sinter. 43 (2011) 277–287.

[7] Finlay D. Morrison, Derek C. Sinclair, and Anthony R. West, Characterization of Lanthanum-Doped Barium Titanate Ceramics Using Impedance Spectroscopy, J. Am. Ceram. Soc., 84 [3] 531–38 (2001).

[8] S. Filipović, N. Obradović, V.B. Pavlović, M. Mitrić, A. Đorđević, M. Kachlik, K. Maca, Effect of consolidation parameters on structural, microstructural and electrical properties of magnesium titanate ceramics, Ceramics International 42 (2016) 9887–9898.

[9] S.-H. Lee, E.R. Kupp, A.J. Stevenson, J.M. Anderson, G.L. Messing, X. Li, E. C. Dickey, J.Q. Dumm, V.K. Simonaitis-Castillo, G.J. Quarles, Hot isostatic pressing of transparent Nd:YAG ceramics, J. Am. Ceram. Soc. 92 (2009) 1456–1463.
[10] K. Maca, M. Trunec, R. Chmelik, Processing and properties of fine-grained transparent $MgAl_2O_4$ ceramics, Ceram. Silikáty 51 (2007) 94–97
[11] A. K. Singh, A. Dhillon, T. D. Senguttuvan, A. M. Siddiqui, Synthesis, Characterization and DC Conduction Mechanism in Inverse Spinel Compound (Mg_2TiO_4), International Journal of Current Engineering and Technology 4 (2014) 399-404.
[12] J. Bernard, D. Houivet, J. El Fallah, J. M. Haussonne, $MgTiO_3$ for Cu base metal multilayer ceramic capacitors, Journal of the European Ceramic Society 24 (2004) 1877–1881.
[13] J. Bernard, F. Belnou, D. Houivet, J. M. Haussonne, Low sintering temperature of $MgTiO_3$ for type I capacitors, Journal of the European Ceramic Society 25 (2005) 2779–2783.
[14] J. R. Macdonald, Impedance Spectroscopy: Emphasizing Solid Materials and Systems, Wiley, New York, 1987
[15] H. Zhu, X.-J. Kuang, C.-H. Wang, H.-T. Xia, L. Li, P. Hu, X.-P. Jing, Z.-X. Tang, F. Zhao, Z.-X. Yue, Annealing effects on conductivity and microwave dielectric loss of $MgTiO_3$ Ceramics, Jpn. J. Appl. Phys. 50 (2011) 065806-065806-5.
[16] X. Kuang, X. Jing, Z. Tang, Dielectric loss spectrum of ceramic $MgTiO_3$ investigated by AC impedance and microwave resonator measurements, J. Am. Ceram. Soc.89 (2006) 241–246.
[17] P. Gogoi, P. Srinivas, Pramod Sharma, D. Pamu, Optical, Dielectric Characterization and Impedance Spectroscopy of Ni-Substituted $MgTiO_3$ Thin Films, Journal of Electronic Materials 45 (2016) 899-909.
[18] A. K. Jonscher, The “universal” dielectric response, Nature 267 (1977) 673-679.
[19] K. Funke, Jump relaxation in solid electrolytes, Prog. Solid State Chem. 22 (1993) 111-195.

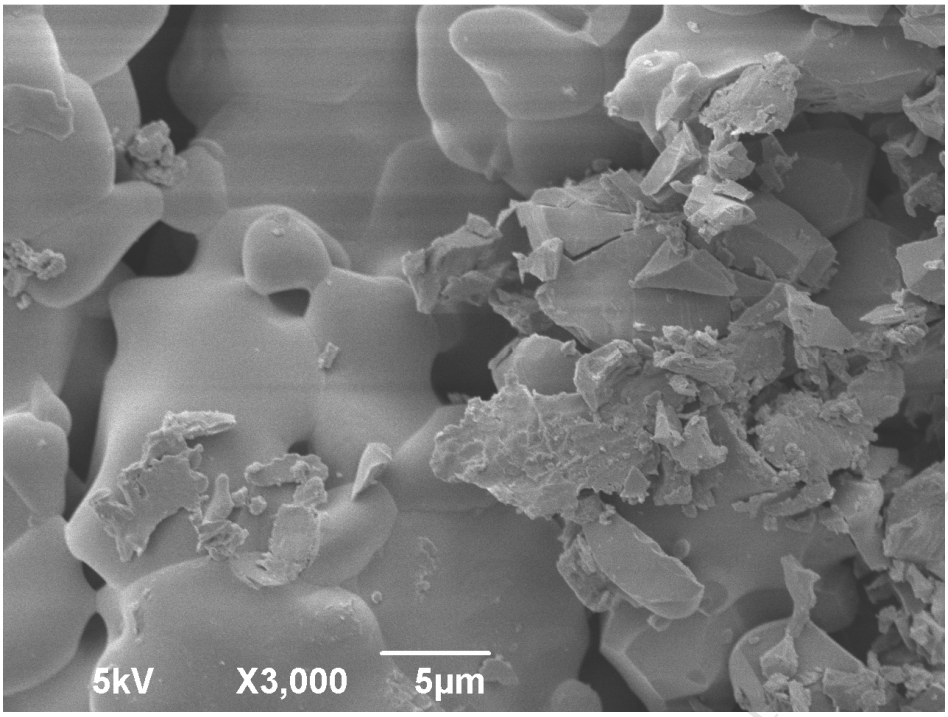

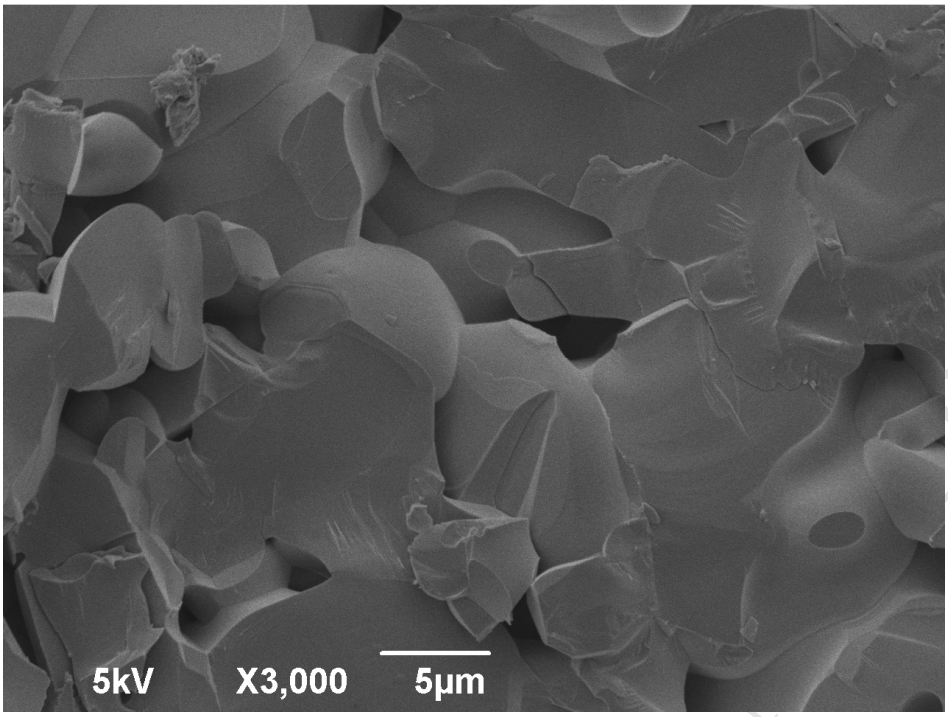

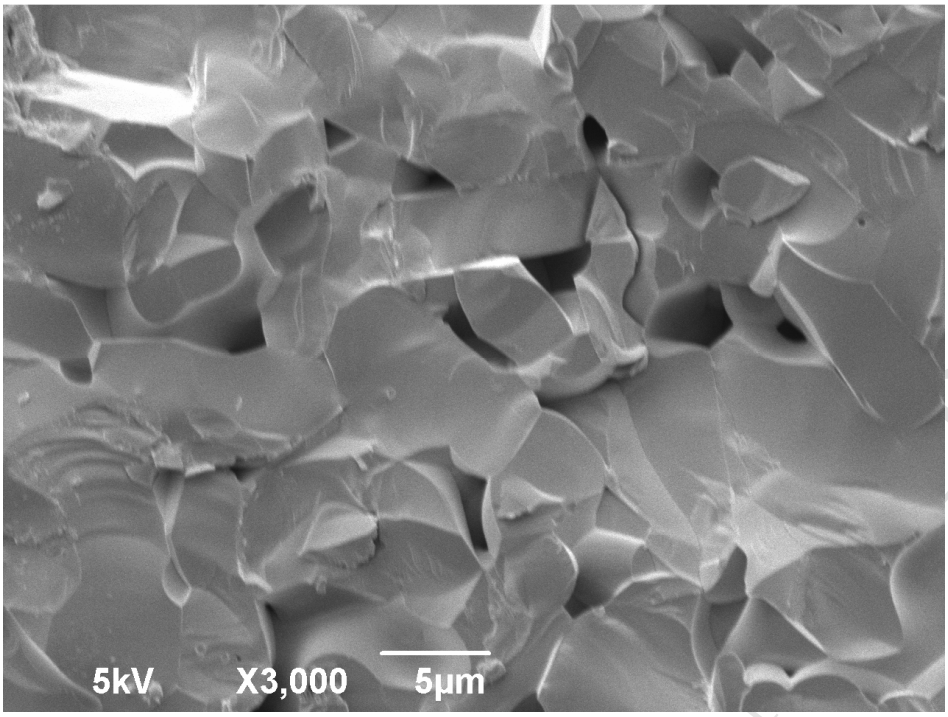

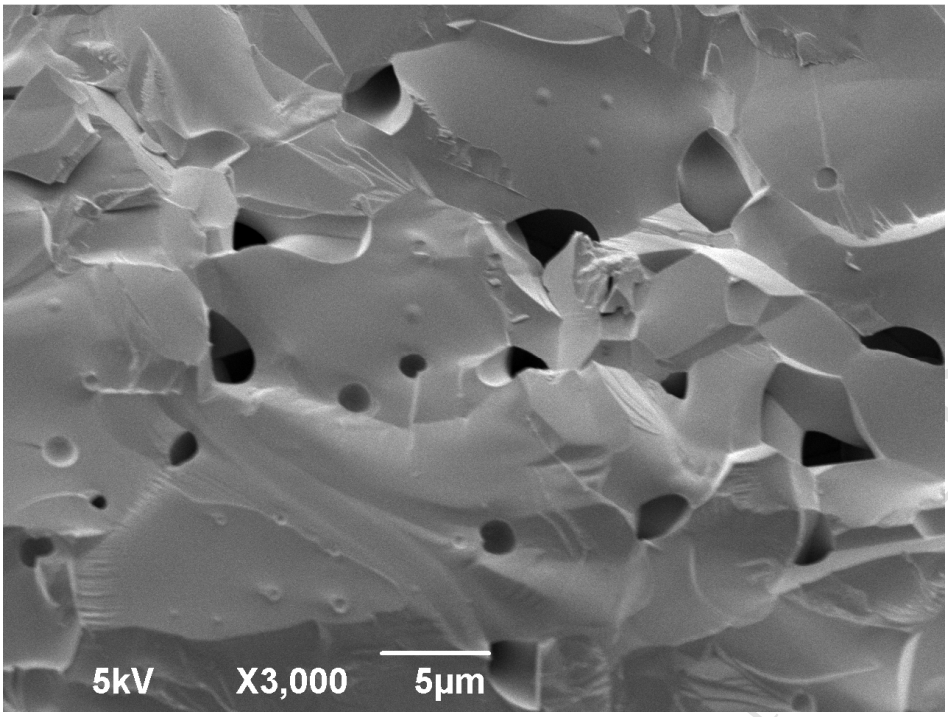

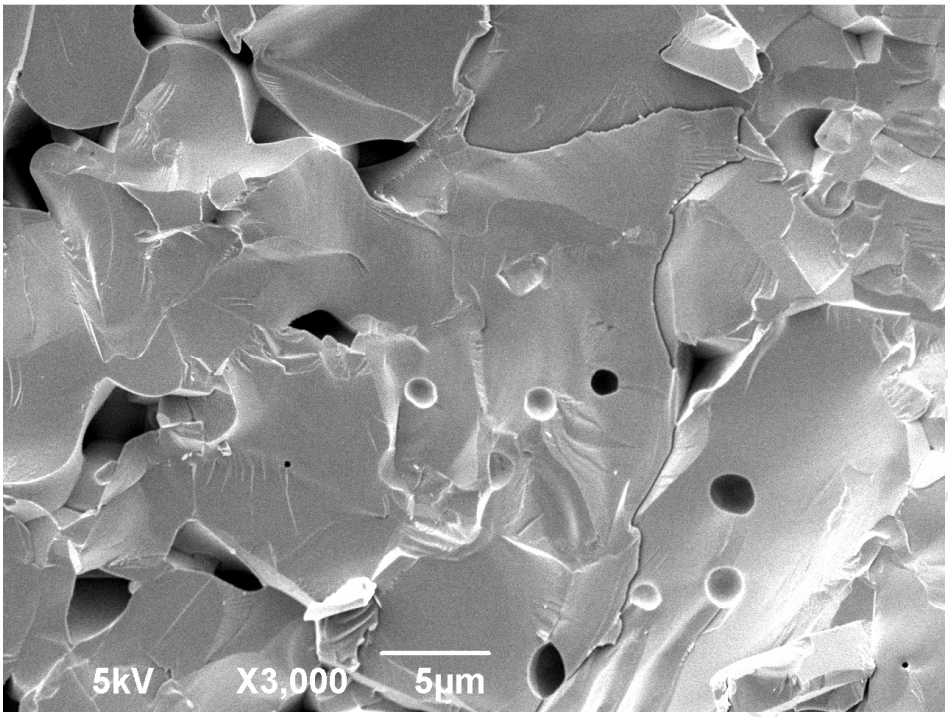

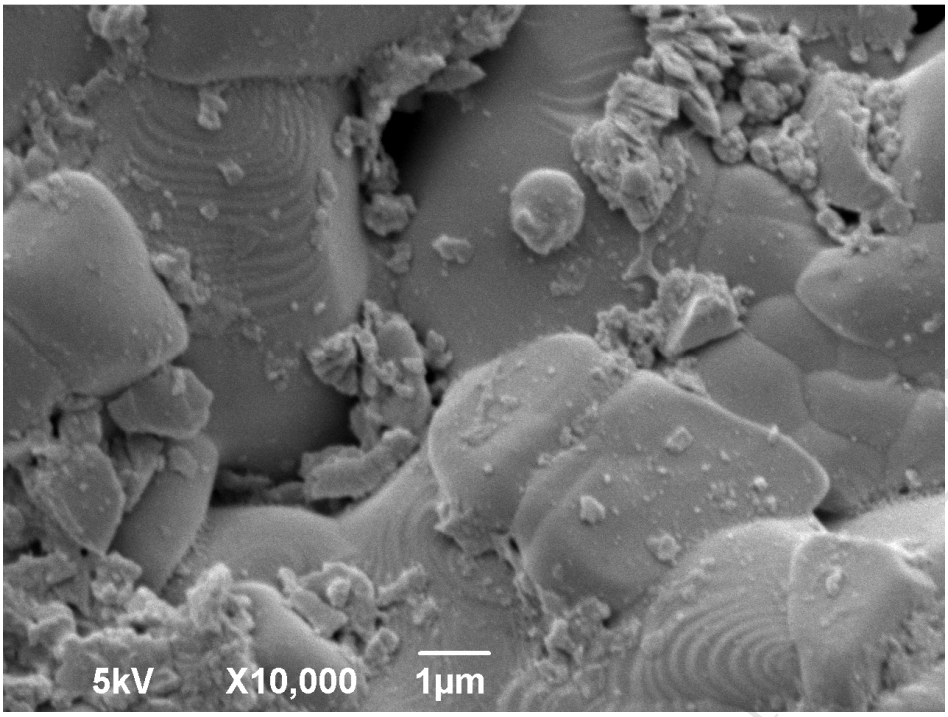

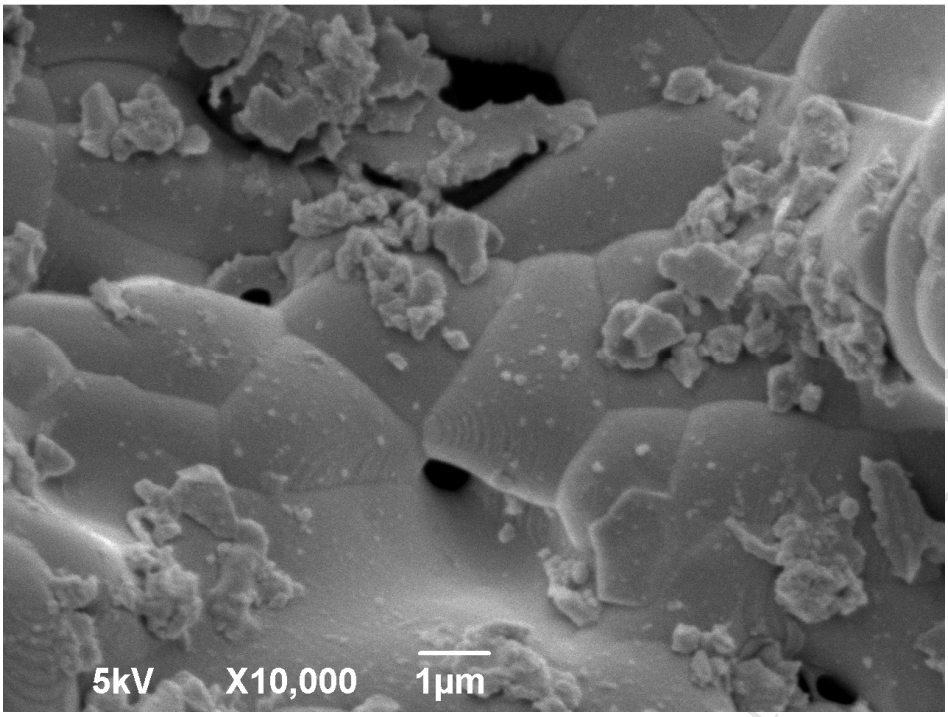

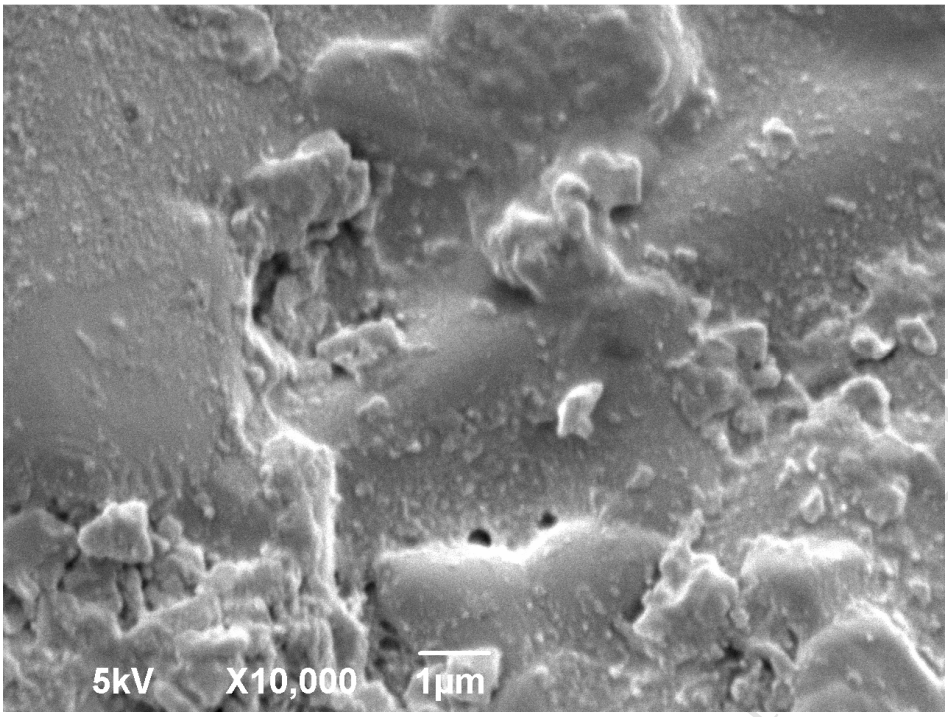

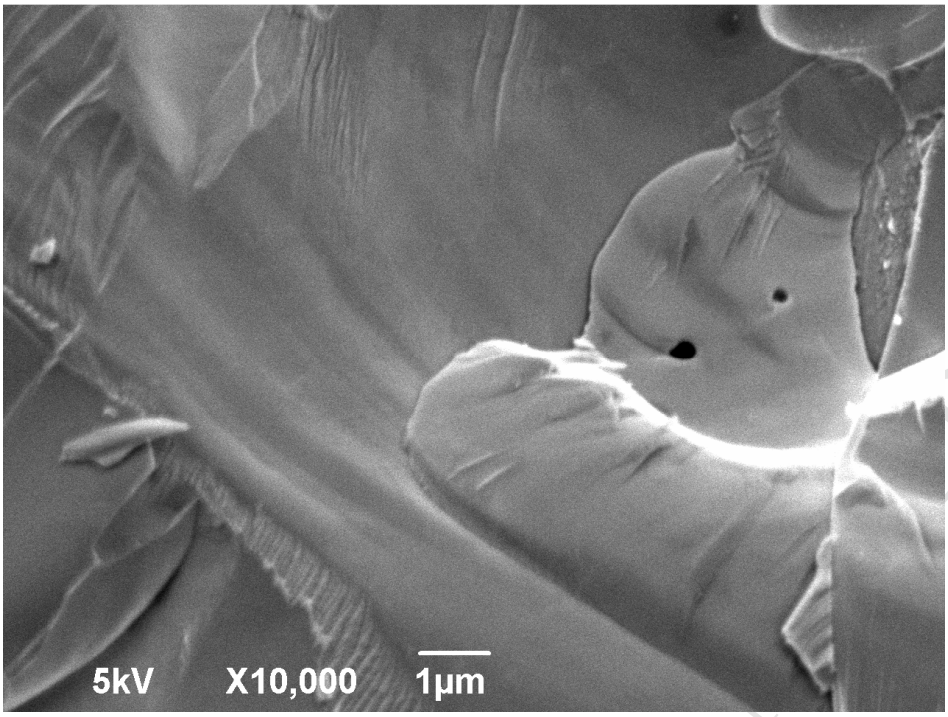

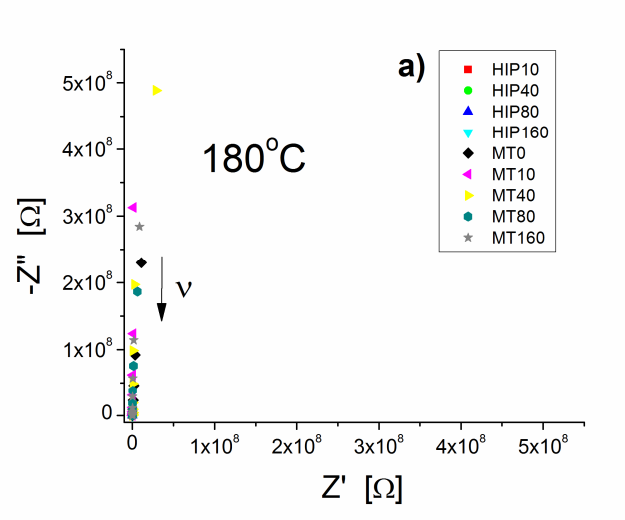

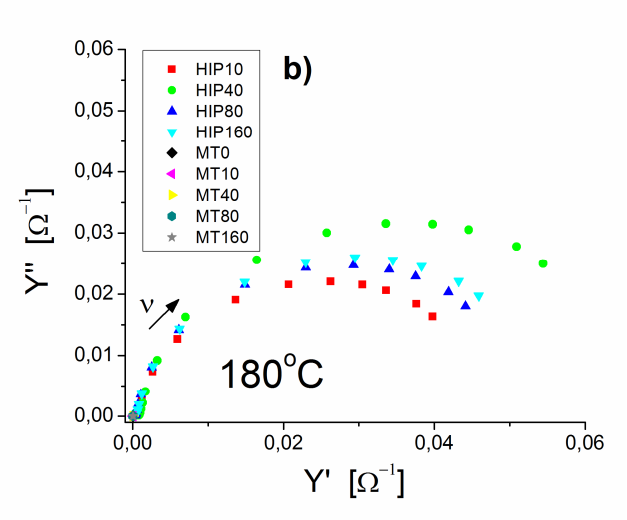

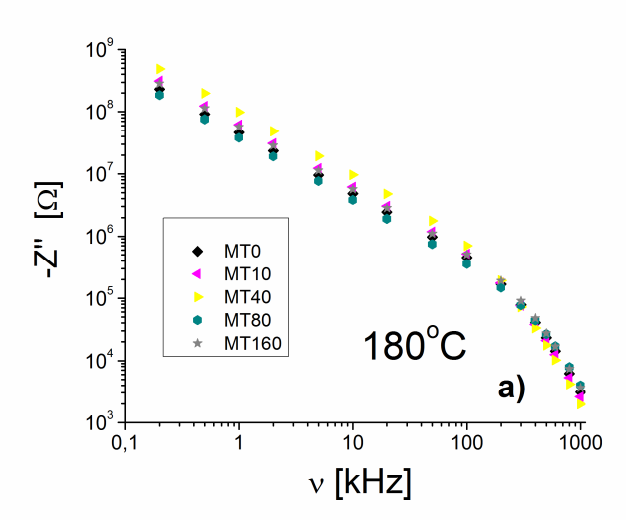

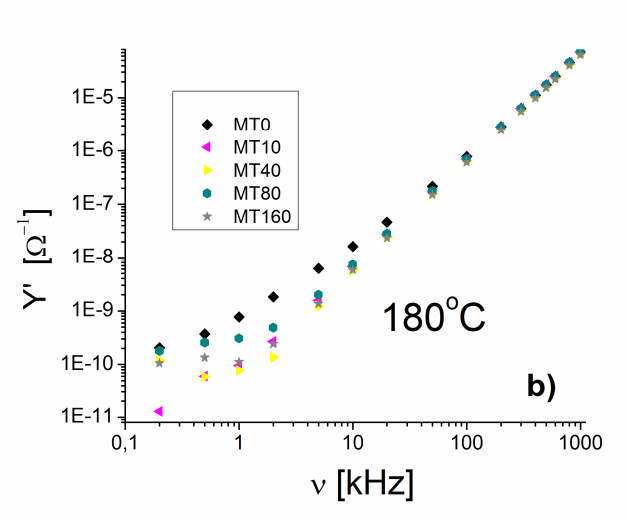

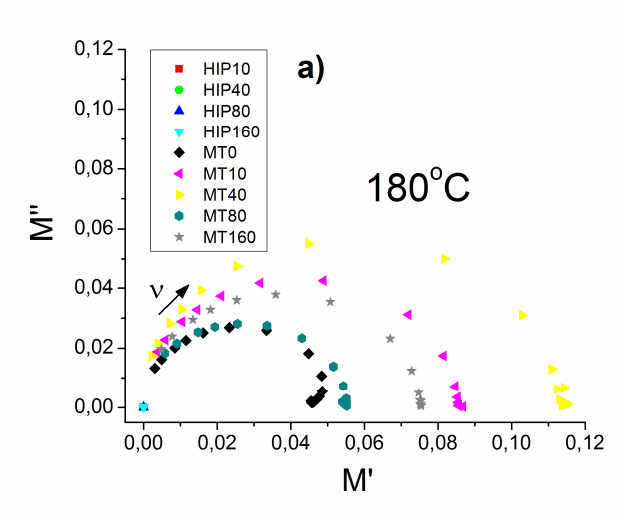

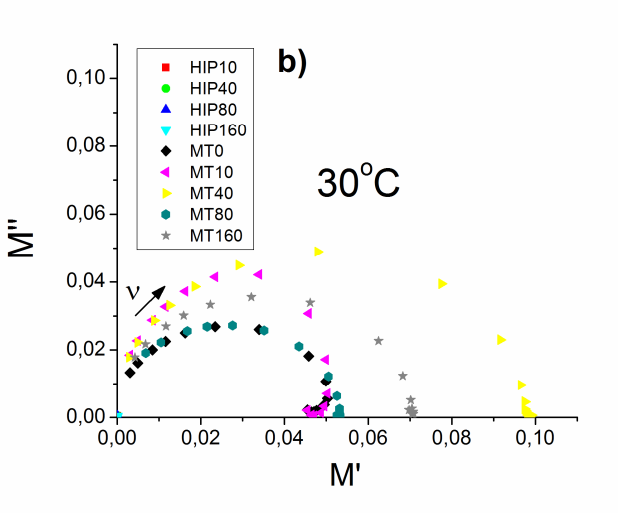

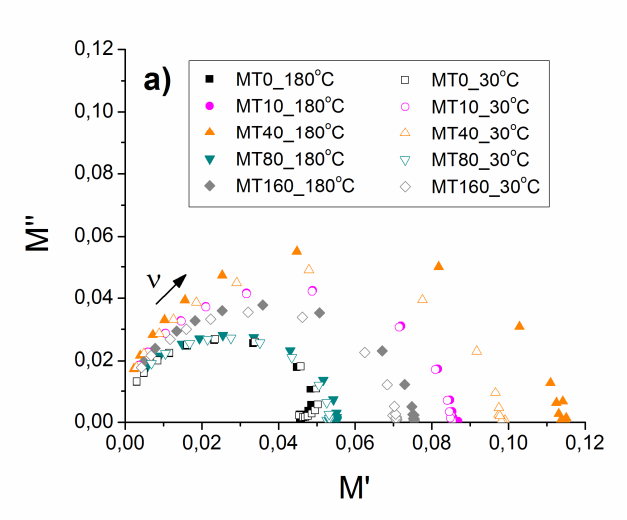

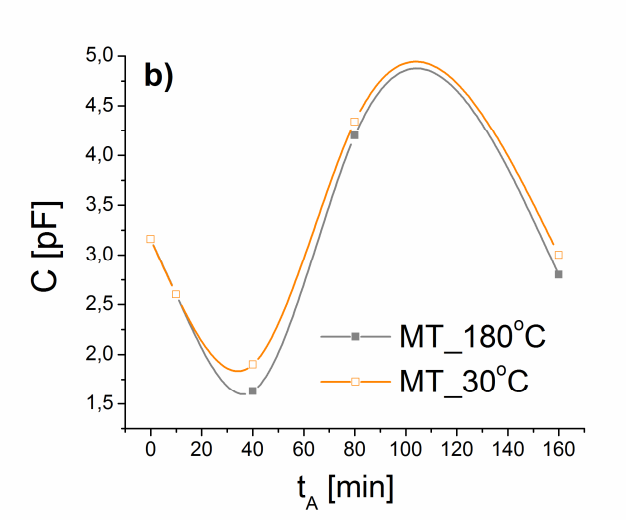

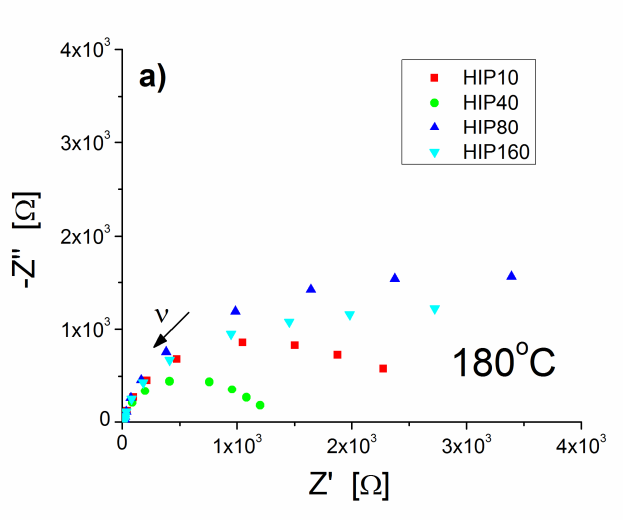

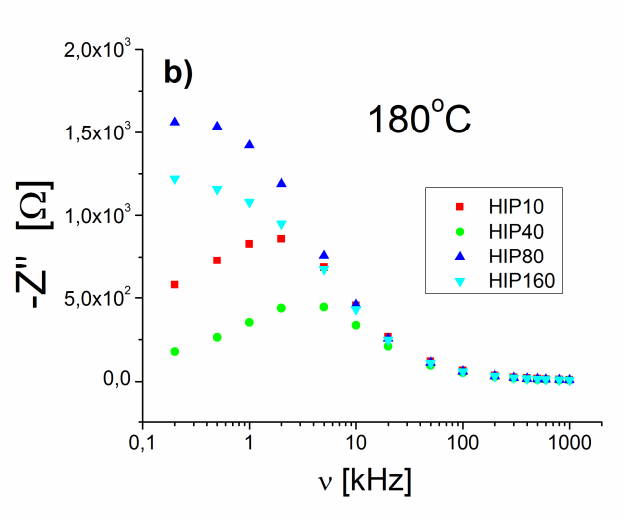

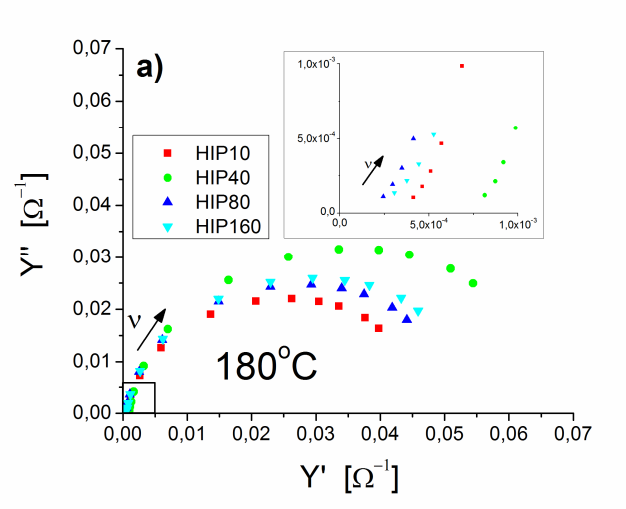

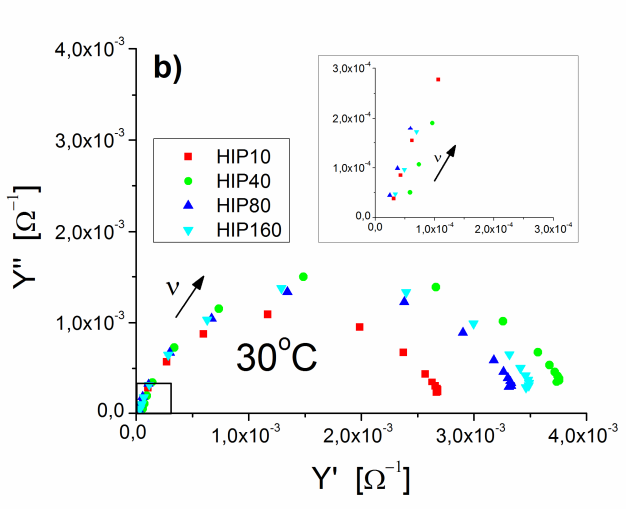

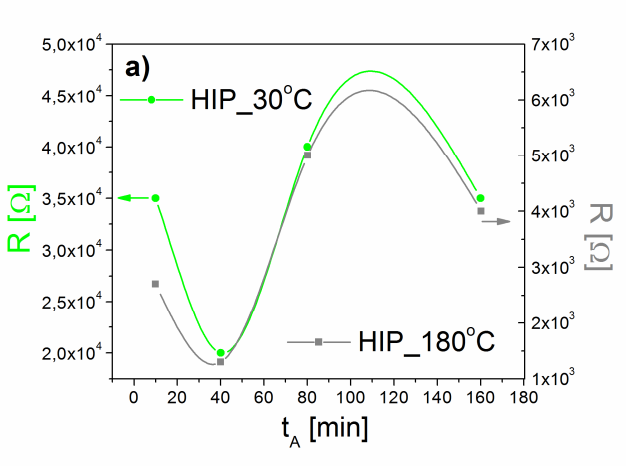

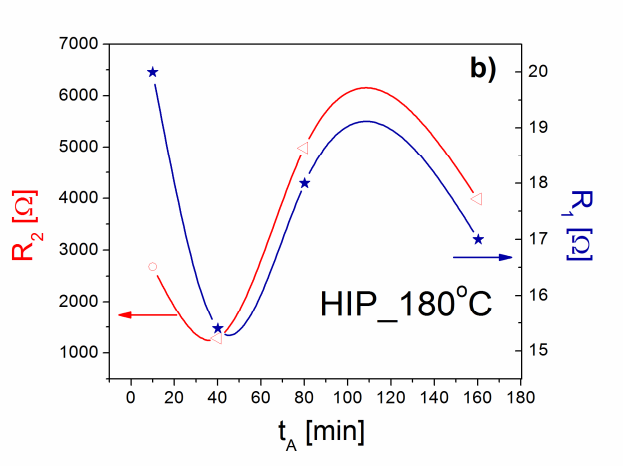

Figure. 1. Scanning electron micrographs of MT samples: a) MT0, b) MT10, c) MT40, d) MT80, and e) MT160.

Figure. 2. Scanning electron micrographs of HIP samples: a) HIP10, b) HIP40, c) HIP80, and d) HIP160.

Figure 3. Plots in: a) Z* plane (Nyquist plots), and b) Y* plane, for all sintered samples.

Figure 4. Frequency dependence of: a) imaginary part of the complex impedance, b) real part of the complex admittance, at 180 ^{o}C, for two step sintered samples (MT0-MT160).

Figure 5. Plots in M* plane for MT and HIP samples at: a) 180 ^{o}C, and b) 30 ^{o}C.

Figure 6. a) Plots in M* plane for MT samples at 180 ^{o}C and 30 ^{o}C, and b) the capacitance of MT samples at 30 ^{o}C and 180 ^{o}C vs. activation time.

Figure 7. a) Plots in Z* plane (Nyquist plots), and b) frequency dependence of imaginary part of electrical impedance, for HIP sintered samples at 180 ^{o}C.

Figure 8. Plots in Y* plane for HIP sintered samples at: a) 180 ^{o}C and b) 30 ^{o}C. Insets represent enlarged view of the results in the low frequency range.

Figure 9. a) Total resistance of HIP sintered samples as a function of activation time, b) the grains and grain boundaries resistance contribution for the HIP samples at 180 ^{o}C vs. activation time.

Figure 10. The influence of temperature on the diagrams in Z* and Y* planes for samples HIP10 and HIP40. Insets represent enlarged view of the results in the low frequency range.

Figure 11. a) Dependence $\ln R = f(1/T)$ for activated and HIP sintered samples, b) The frequency dependence of conductivity for HIP samples at 180 ^{o}C (b).

Figure 12. Plots in: a) M* plane, and b) ε_r * plane, for HIP sintered samples at 180 ^{o}C. Inset represents enlarged view of the results in the high frequency range, c) the contribution of grain boundary capacitance for the HIP sintered samples at 180 ^{o}C vs. activation time.

Figure 13. Frequency dependence of imaginary part of complex electric modulus for HIP10-HIP160 samples, measured at 180 ^{o}C.

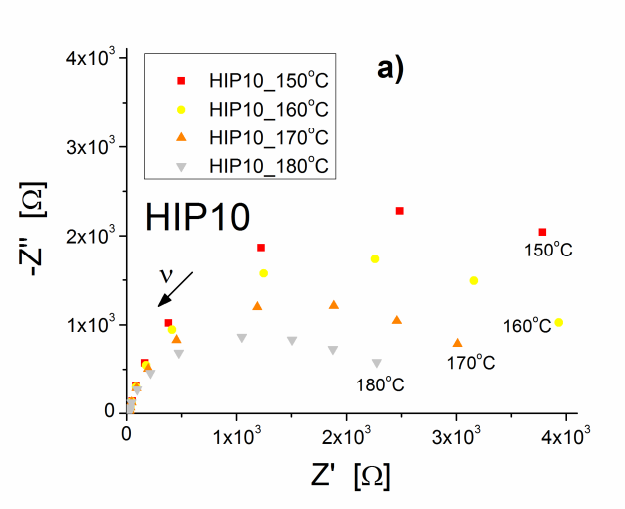

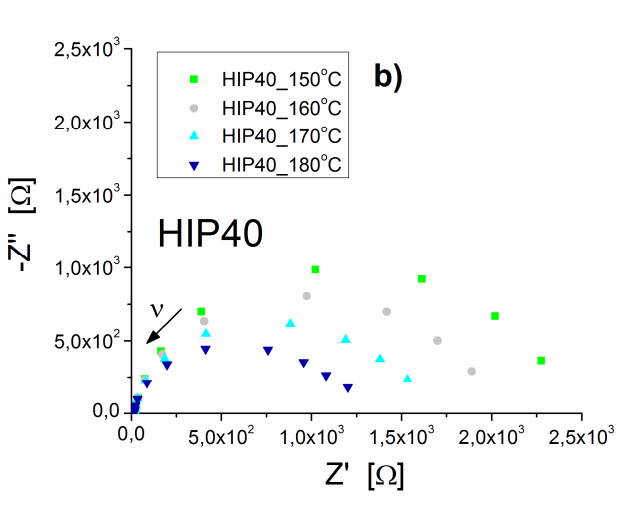

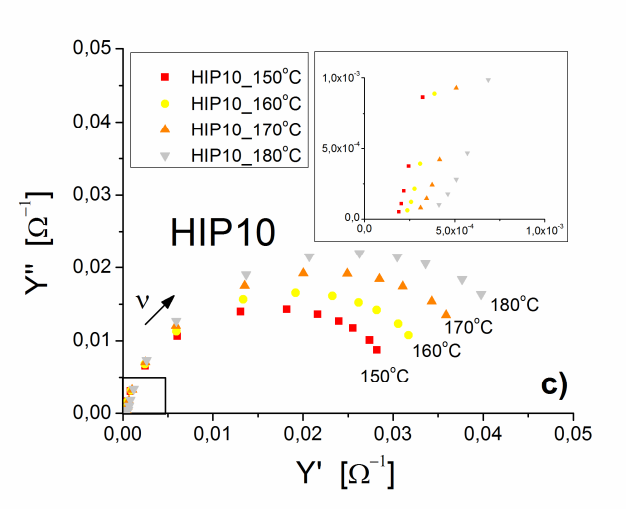

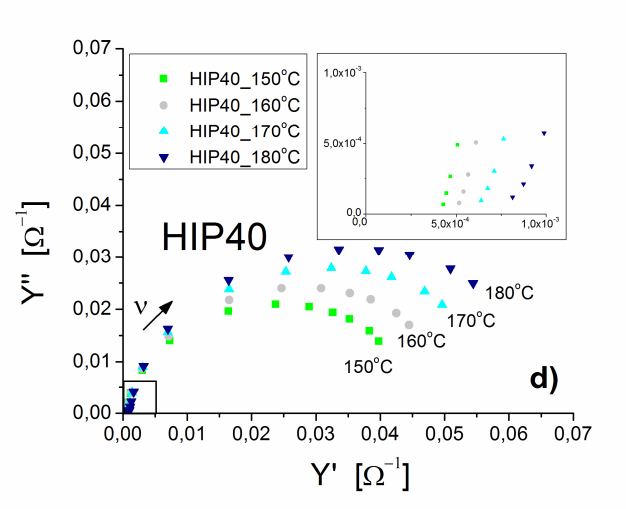

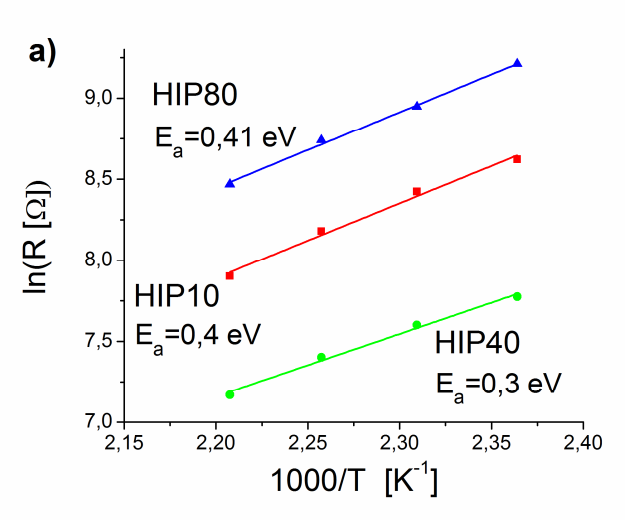

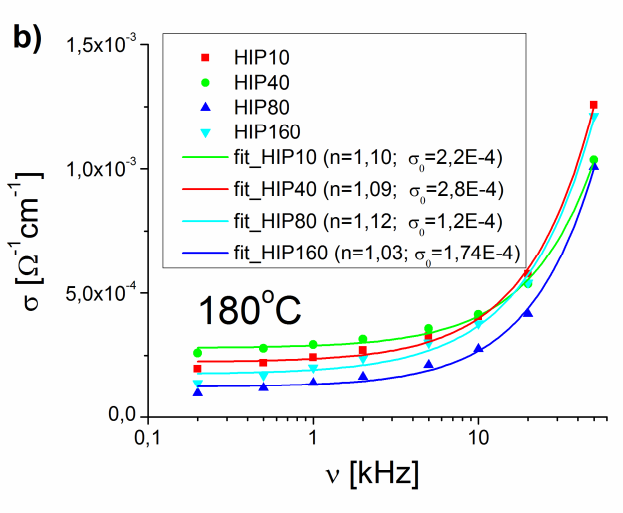

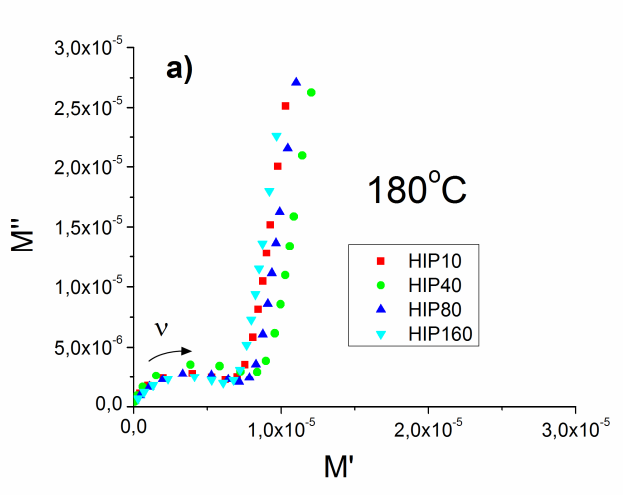

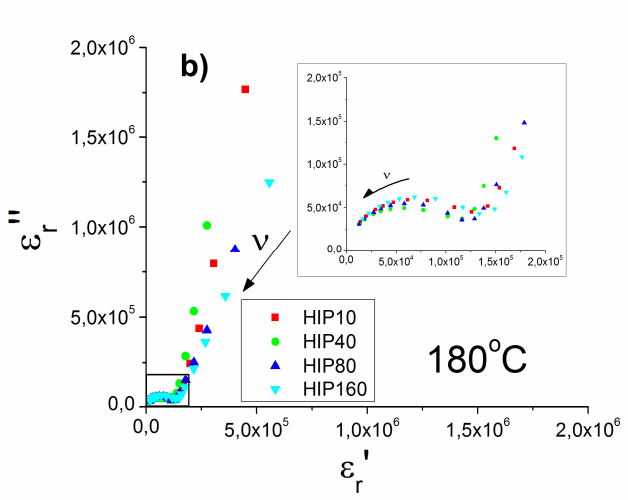

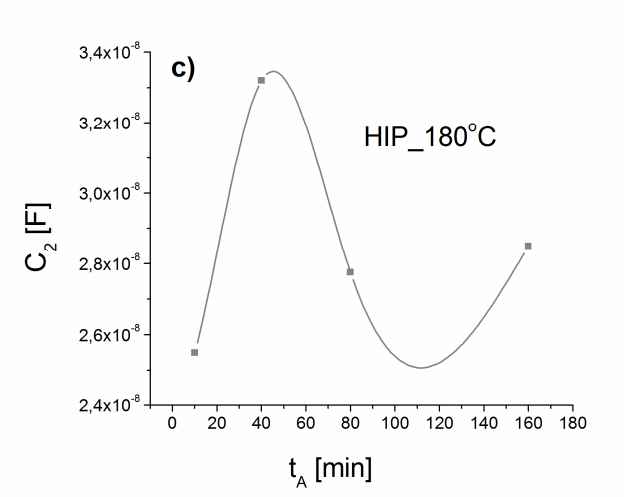

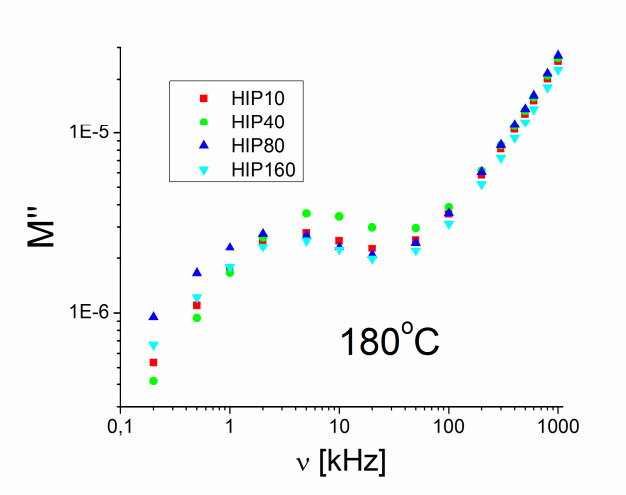

The micrographs of two-step sintered samples indicated the increase in transport mass

Impedance analysis showed that the total resistance is of the order of 10 GΩ

The capacitance of MT samples decreases for the activation up to 40 min

HIP sintered samples show totally different behavior in the electrical properties

Degree of disorder in crystal structure influences the process of thermal conductivity